

# NUMERICAL SIMULATION OF IN-FLIGHT AIRCRAFT ICING

M.T. Brahim<sup>\*</sup> P. Tran<sup>†</sup> F. Tezok<sup>‡</sup> I. Paraschivoiu<sup>§</sup>

*Department of Mechanical Engineering, École Polytechnique de Montréal  
C.P. 6079, Succ. Centre-Ville, Montréal, Qc, Canada, H3C 3A7*

*<sup>‡</sup>Advanced Aerodynamics Section, Bombardier Inc./Canadair  
400 Côte-Vertu, Dorval, Qc, Canada, H4S 1Y9*

## Abstract

The present paper outlines progress in the development of a numerical code for the Canadian aerospace industry to simulate ice accretion on single airfoils (*CANICE*) and multi-element airfoils (*CANICE-ME*). The flow field calculation about the airfoil is based on Hess and Smith panel method and the droplet equation of motion is derived from Newton's law and takes into account the buoyancy, drag and gravitational forces. Thermodynamic characteristics of the freezing process of the incoming liquid water is taken into account by considering the mass and energy balance on the body surface. *CANICE* code has been tested on NACA 0012 airfoil as well as on supercritical airfoils for typical business jets. It has also been extended to handle ice accretion prediction on wings using the equivalent angle of attack method as well as ice accretion due to supercooled large droplets (SLD). The present study shows that ice shapes can be predicted on multi-element airfoils using the same technique as for single element airfoils. Currently, further work is under consideration to validate the *CANICE-ME* code with available experimental data.

## Nomenclature

$c$	:	chord, $m$
$C_D$	:	drag coefficient
$\vec{g}$	:	gravitational acceleration, $m/s^2$
$h$	:	convective heat transfer, $W/(m^2 \text{ } ^\circ C)$
$k_s$	:	roughness height, $m$
LWC	:	liquid water content, $g/m^3$
$\dot{m}$	:	mass flow rate, $kg/s$
$D$	:	droplet diameter, $m$
$\vec{r}$	:	droplet position, $m$
$Re$	:	Reynolds number
$T$	:	temperature, $^\circ C$
$V$	:	velocity, $m/s$

<sup>\*</sup>Research Associate

<sup>†</sup>Ph.D. Student

<sup>‡</sup>Staff specialist

<sup>§</sup>Bombardier Aeronautical Chair Professor

## 1 Introduction

New aircraft designs incorporating advanced and modified control and lifting surfaces have presented the Federal Aviation Administration with new certification and flight safety assessment issues. These effects are particularly significant, from the safety point of view, and require demonstration that the aircraft can operate safely under all atmospheric and flight conditions which fall within the intersection of operating envelope of the aircraft and the atmospheric icing envelope of the Federal Aviation Regulation. Investigation of aircraft crashes due to wing contamination indicates that for the safe operation of an aircraft, current regulations applicable to ice, frost or snow accumulation might not be effective in preventing aircraft icing accidents <sup>(1,2)</sup>. Test data on ice effects indicate that the formation of ice, snow, or frost on unprotected wing can lead to a number of aerodynamic degradation problems <sup>(3)</sup>. A reduction of wing lift by as much as 30% and drag increase by 40% are the result of such contamination when thickness and surface roughness are similar to medium or coarse sandpaper <sup>(4,5)</sup>. To overcome these penalties, various practical methods have been used to remove or prevent accumulation of ice on aircraft surfaces by applying de-icing/anti-icing procedures <sup>(6)</sup>. However, failure of protection systems and the presence of residual ice still produce a loss in the aircraft efficiency. In addition, modern airfoils using new materials have been developed and have demonstrated a high aerodynamic efficiency. But, at the same time, these new types of airfoils need specific ice protection systems to maintain their aerodynamic efficiency and safety margin. The design of such system will require efficient optimization of ice protection systems, accurate modeling of ice accretion and its removal from critical surfaces.

The present paper presents the development of (*CANICE*) and (*CANICE-ME*) codes to simulate ice accretion on single and multi-element airfoils.

## 2 Background

During the last decade many theoretical and experimental studies have been conducted to investigate ice accretion on an aircraft operating in natural icing conditions<sup>(3,7)</sup>. To prevent icing-related accidents, various practical methods have been used; however failure of protection systems and the necessity of flight in icing areas have stimulated new research effort on aircraft icing. Presently, one of the most important steps that needs to be taken is to understand the micro-physical processes of ice accretion. Surface roughness, boundary-layer transition, separated flow at the stall and post-stall angle, local heat transfer, collection efficiency and de-icing/anti-icing fluid behaviour are the major parameters that should be considered for a realistic understanding of ice accretion mechanisms. Several researchers<sup>(3,8)</sup> have developed 2-D and 3-D models to predict ice accretion on aircraft components and to calculate the aerodynamic characteristics of lifting and non-lifting surfaces with ice including NASA<sup>(9)</sup>, DRA (England)<sup>(10)</sup>, ONERA (France)<sup>(11)</sup> and Bombardier Chair (Canada)<sup>(2)</sup> programs. These significant studies started with the work of Bragg<sup>(12)</sup>, Lozowski and Oleskiw<sup>(13)</sup>, Frost *et al.*<sup>(14)</sup> and Cansdale and Gent<sup>(15)</sup>. A mathematical model of glaze and rime ice accretion on a 2-D airfoil was presented by MacArthur *et al.*<sup>(16)</sup>. In 1985 Bragg<sup>(17)</sup> improved his previous model, derived a method to solve the droplet trajectories and impingement characteristics and gave some recommendations for further improvement of the method. In the light of these developments, more experimental and theoretical investigations of icing have been performed by many researchers such as Fleming and Lednicer<sup>(18)</sup>, Cebeci<sup>(19,20)</sup>, Bragg and Khodadoust<sup>(21)</sup>. A very large research program on aircraft icing is being conducted by NASA Lewis Research Center. A 2-D ice accretion model, *LEWICE*, was developed in 1983 at the University of Dayton Research Institute and later modified by Ruff and Berkowitz<sup>(22)</sup>. The original *LEWICE* code based on potential flow analysis, is capable of calculating the shape of the ice accretion on the airfoil under rime ice conditions. This code has been modified by Cebeci *et al.*<sup>(23)</sup> to include viscous effects by using potential flow with Interactive Boundary Layer, *LEWICE/IBL*. The effect of compressibility has been incorporated by Potapczuk<sup>(24)</sup> in the so-called *LEWICE/E* code which is an inviscid compressible flow ice accretion code based on solving the Euler equation for the flow field flow analysis. Potapczuk *et al.*<sup>(25)</sup> extended the original *LEWICE* program by using the solution of the 2-D Navier-Stokes equations in the *LEWICE/NS* code which includes a module for grid generation, predicts the flow field, calculates droplet trajectories and the shape of ice accretions based on energy balance calculations and predicts aerodynamic characteristics.

Potapczuk *et al.*<sup>(26)</sup> also developed a 3-D version of *LEWICE* for swept wings. Other computer codes are also available at the NASA Lewis Research Center including *LEWICE/T* which is a program with conduction for electrothermal de-icer modelling capability, *LEWICE/TNG* which is a program with an improved ice physics model (Wright<sup>(27)</sup>). Kwon and Sankar<sup>(28)</sup> developed a 3-D compressible Navier-Stokes solver for studying the glaze ice accretion effects on the sectional and total aerodynamic characteristics of a finite 3-D wing. The numerical calculations have been performed on a clean and iced untwisted and untapered wing having a NACA 0012 airfoil section and an aspect ratio of 5. A premature stall for an iced wing is observed even at 8° angle of attack which leads to a significant reduction of the lift. The model of Kwon and Sankar is able to predict well the locally separated flow region at the iced wing leading edge but the results are not accurate for a massively separated flow. A very important study involving detailed experimental observations of accreting ice surfaces has been conducted by Hansman<sup>(29)</sup> at MIT. This work included observation of physical mechanism including behaviour of the liquid flow over the ice surface, development of roughness and its effects on heat transfer, and the development of "feather" formation in certain zones. An interesting research program for predicting the ice accretion has also been developed by Guffond<sup>(30)</sup> at ONERA for the 2-D case and by Hedde and Guffond<sup>(31)</sup> for the 3-D case. In the 3-D model, the authors used a finite volume compressible boundary layer laminar/turbulent code developed at ONERA/CERT<sup>(31)</sup> for non separated flows. An icing research program by DRA in England has also developed a number of 2-D icing codes (Gent<sup>(32)</sup>) especially for helicopter rotor blades and for ice protection of airfoils. Currently several ice accretion codes exist in the international aircraft icing community *LEWICE* (U.S.A.), *ONERA* (France), *DRA* (United Kingdom), *CANICE* (Canada) and more recently *CIRA* (Italy). In Canada, Canadair has initiated a research and development program with École Polytechnique to develop a computer code for calculation of ice accretion on single and multi-element airfoils<sup>(2,33)</sup>. The code developed includes the flowfield calculation, integration of particle trajectories, thermodynamic analysis and geometry update with the possibility to study the effect of several parameters that influence ice formation such as ambient temperature, roughness height, liquid water content, accretion time, droplet diameter, etc.

## 3 In-Flight Icing Mechanism

The formation of ice on aircraft components such as wings, control surfaces and engine intakes occurs when the aircraft flies at a level where the temperature is

at, or slightly below the freezing point and the atmosphere contains supercooled water droplets. When the water droplets are hit by the aircraft they begin to freeze immediately. As the water freezes, heat is released so that their temperature rises until they reach  $0^{\circ}\text{C}$ . As this temperature is reached, freezing stops while the remaining liquid fraction of the droplets starts to run back along the surface of the aircraft or along existing ice. The rate of heat loss from the aircraft surfaces is such that some or all of the droplets are frozen before they can run off the body.

Two basic conditions must be met for ice to be formed: the ambient temperature must be below  $0^{\circ}\text{C}$  and supercooled water droplets must be present. Aircraft can experience icing in temperatures ranging from  $0^{\circ}\text{C}$  to  $-40^{\circ}\text{C}$  and icing is usually restricted to the lower 10,000 m of the troposphere (900 to 10,000 m). The more dangerous types of ice are encountered in dense clouds, composed of heavy accumulations of large water droplets.

There are two basic types of clouds, the stratiform clouds with a large horizontal extent having a low liquid water content ( $LWC = 0.1$  to  $0.9\text{ g/m}^3$ ), and the cumuliform clouds with a small horizontal extent but having a higher liquid water content (up to  $3\text{ g/m}^3$ )<sup>(34,35)</sup>. The amount and the shape of ice collected depend mainly on liquid water content, temperature, airspeed, droplet size and surface roughness. Two basic types of ice can be formed, rime ice, if all the impinging water droplets freeze upon impact, or glaze ice if only a fraction of the water droplets freezes while the remainder runs back along the body surface. Rime ice is a dry, opaque and milky white ice deposit that usually occurs at low airspeed, cold temperature and low liquid water content. It is characterized by the instantaneous freezing of small supercooled water droplets as soon as they hit the surface of the aircraft. There is virtually no spreading from the point of impact, there is a tendency for trapping the air within the ice structure. The deposit has an effect on the aerodynamic characteristics of the wing but is brittle and can be removed using anti-icing/de-icing equipment. In contrast, glaze ice (or clear ice) is a wet growth ice formed from the partial freezing of large supercooled droplets. Glaze ice occurs at a warmer temperature (near freezing) and relatively high liquid water content. It has a density closer to that of the cloud water ( $917\text{ kg/m}^3$ ) indicating the wet nature of its formation. It is a heavy coating of glassy ice which has a clear appearance. The glaze ice accretion process produces different ice deposit shapes, double horned, beak or rounded glaze ice shapes are possible. This type of ice dangerously affects and alters the shape of the original body surface, resulting in aerodynamic penalties much more severe than those typically due to rime ice accretion. Hence, the most

dangerous icing develops when the ambient temperature is at or slightly below freezing point and the aircraft flies through a region where the liquid water content is high and droplets are large. Results from wind tunnel and flight icing tests indicate that ice accretion on aircraft components can lead to a number of aerodynamic degradation problems and consequently is a major safety problem<sup>(3,36,37)</sup>. The most severe penalties encountered are due to decreased maximum lift, increased drag, decreased stall angle, changes in the pressure distribution, early boundary-layer transition, increased stall speed and reduced controllability.

## 4 Numerical Simulation of Icing

The main objective of ice simulation is the calculation of the impingement of the particles on the airfoil which determines the droplet impingement regions as well as the mass of liquid on the body surface. The main applications are for use as input to ice accretion calculation, to predict aerodynamic performance degradations, and for use in the design of anti/de-icing systems. The computational procedure is an iterative process with a time-stepping procedure where successive thin ice layers are formed on the surface and followed by flow field and droplet impingement recalculations. The flow field calculation provides the velocity field at the airfoil surfaces as well as at any point in the field away from the surface. The droplet trajectories are determined by solving the equation of motion to obtain the entire path for each droplet moving in the flow field and hitting the wing. Once the trajectory paths are known, the droplet impingement limits as well as the global and local collection efficiencies can be calculated using an efficient scan procedure of the frontal surface of the wing. The calculation of the water flux impinging on each panel forming the wing surface can be performed, then the ice accretion is calculated and the geometry is modified defining the ice shape for the first time step. The procedure is then performed for another time step to calculate a new ice layer.

### 4.1 Flow Field Calculation

While some authors<sup>(38,39)</sup> used Navier-Stokes calculations to get flow field velocities, it is believed that no additional accuracy is provided<sup>(40)</sup>. This is due to the use of empirical models to solve energy balance and to the limited understanding of surface roughness with ice. As a consequence, it is more convenient to use a simple model, such as panel method, to calculate the flow field velocities and then perform droplet trajectories. In the case of multi-element airfoils, an extension of the Hess & Smith panel method<sup>(41)</sup> to multiple element configurations has been developed. For the flow field calculation over the wings, a fully

three-dimensional model based on Viscous-Inviscid Interaction techniques <sup>(42)</sup> has been used to determine the sectional lift coefficient,  $C_{L3D}$ , along the different wing stations, then an equivalent two-dimensional angle of attack,  $\alpha_{2D}$ , as suggested by Chen *et al.* <sup>(43)</sup>, is calculated which produces the same sectional lift coefficient (*i.e.*  $C_{L3D}$ ). The Viscous-Inviscid Interaction technique involves: a panel method, a boundary layer correction and a suitable matching procedure using the transpiration velocity model.

## 4.2 Droplet Trajectory Calculation

To obtain the resulting ice shape, droplets are released upstream of the wing and followed until impact on the surface. The droplet equation of motion takes into account the drag, buoyancy and gravitational forces. At each integration step, the local velocity needed to solve the droplet equation of motion is obtained from the flow field solution while the integration is continued following droplets until they impinge on the wing surface or pass downstream of the wing. The droplet equation of motion is given by

$$\frac{d^2 \vec{r}_d}{dt^2} + \frac{C_{D_a} R_e}{24} \frac{1}{K_A} \frac{d \vec{r}_d}{dt} = K_G + \frac{C_{D_a} R_e}{24} \frac{1}{K_A} \vec{V}_a \quad (1)$$

where  $K_G = \frac{(\rho_a - \rho_w)g}{\rho_a}$  and  $K_A = \frac{\rho_a D_d^2}{18 \mu_a}$ . The droplet trajectory equation represents a second order differential equation which can be solved using classical difference methods. The drag force is determined using steady-state drag coefficient for a sphere which is a function of Reynolds number. Two correlations were determined: one for small droplets ( $\leq 40 \mu m$ ) and one for large droplets (up to  $2000 \mu m$ ).

## 5 Thermodynamic Analysis

The next step is to perform a thermodynamic analysis on the surface of the wing. The model is based on the first law of thermodynamics which states that the mass and energy must be balanced in a control volume on the surface. Based on the heat balance and the mass flux, the fraction of the freezing water droplets on each control volume can be determined. The procedure is repeated for the adjacent control volumes and continued along the entire wing. The mass balance will take into account the mass flow rate of the impinging water,  $\dot{m}_{im}$ , the mass flow rate of water flowing into the control volume (runback water from previous CV),  $\dot{m}_{in}$ , the mass flow rate of water flowing out of the control volume (runback water to next CV),  $\dot{m}_{ou}$ , the mass flow rate due to evaporation or sublimation,  $\dot{m}_{va}$ , and the mass flow rate of the freezing water,  $\dot{m}_{so}$ . The energy balance will take into account the convective heat losses,  $\dot{Q}_c$ , the heat

gain by friction  $\dot{Q}_f$ , the enthalpy associated with impinging water and runback water entering the control volume,  $\dot{H}_{im}$  and  $\dot{H}_{in}$ , the enthalpy associated with evaporation or running back to neighboring control volumes,  $\dot{H}_{va}$  and  $\dot{H}_{ou}$  and finally the internal energy,  $\dot{E}_{so}$  calculated in relation to a given reference state depending on the type of surface involved: dry, wet or liquid. The model developed is based on work by Messinger <sup>(44)</sup>. The continuity and energy equations are given by

$$\dot{m}_{im} + \dot{m}_{in} = \dot{m}_{va} + \dot{m}_{ou} + \dot{m}_{so} \quad (2)$$

$$\dot{E}_{so} + \dot{H}_{va} + \dot{H}_{ou} - \dot{H}_{in} - \dot{H}_{im} = \dot{Q}_f - \dot{Q}_c \quad (3)$$

The heat transfer coefficient,  $h_c$ , is computed from two empirical relations, one for the laminar region and one for turbulent region

$$h_{c,l} = 0.296 \frac{k_a}{\sqrt{\nu}} \left[ u_e^{-2.88} \int_0^s u_e^{1.88} ds \right]^{-1/2} \quad (4)$$

$$h_{c,t} = S_t \rho u_e c_p \quad (5)$$

where  $k_a$  is the thermal conductivity of the air,  $S_t$  the Stanton number, and  $u_e$  is the surface velocity obtained by the flow field calculation. The laminar-turbulent transition is determined using Von Doenhoff criterion <sup>(45)</sup> The specification of the equivalent sand roughness  $k_s$  is either uniform or function of liquid water content, static air temperature and droplet diameter as given by Shin *et al.* <sup>(46)</sup>.

## 6 Multiple Element Icing Simulation

The mathematical and numerical model described in the previous sections has been implemented in the computer program *CANICE-ME* to simulate ice accretion on multi-element configurations. The different modules developed have been kept essentially in the same manner as in the case of single-element airfoil (*CANICE* code) <sup>(33)</sup>. However, to be able to simulate ice on multi-element configurations the flow field and droplet trajectory modules have been changed. The flow field was based on a multi-element panel method which is an extension of the Hess & Smith method <sup>(41)</sup> applied to airfoils with multiple elements. Source and vorticity is distributed on straight-line panels on each element. Influence coefficients are calculated for each element on each element yielding a matrix system. The system is solved using Gauss elimination method yielding the unknown singularity strengths. The pressure and velocity fields are calculated using the singularity strengths.

The droplet trajectory calculation is similar to the method described in reference <sup>(47)</sup>. The difference resides in the sweep procedure modified to determine the

impingement on the droplets on any element of the multi-element airfoil. First, the area defined by the user, upstream of the airfoil, is divided into a number of droplet release points. The code simulates the trajectory of each droplet. The code calculates impacts on the first element. Then, it proceeds similarly for each and every element in the geometry. However, to reduce computational time, each droplet impinging on a given element is eliminated from the sweep for the downstream elements.

## 7 Results and Discussion

### 7.1 Effects of Icing Parameters

The effects of the most influencing parameters have been investigated using the icing codes developed and has confirmed the observations of several authors (3,48). Ice shape is influenced by ambient temperature, liquid water content, angle of attack, freestream velocity, droplet diameter and chord length.

#### 7.1.1 Ambient Temperature

Ambient temperature is perhaps the parameter that has the most influence on the ice accretion process. Its effects are reflected in the resulting shape and type of ice accretion. Usually, low temperatures lead to rime ice structures whereas higher temperatures, near the freezing point, result in glaze ice. The ice shape changes from smooth to horned or beaked shape. As the ambient temperature approaches the freezing point, the impinging water does not freeze on impact, it runs back on the body surface creating irregular shapes. Because of the evaporative process, the total mass of ice accreted decreases with increasing temperature.

#### 7.1.2 Liquid Water Content

The liquid water content (*LWC*) is defined as the mass of liquid water contained in a given volume of air. The mass of ice accreted increases proportionally with *LWC*. However, it does not have an effect on impingement limits which determine the local and global catch efficiencies.

#### 7.1.3 Freestream Velocity

Freestream velocity has large effects on the resulting ice shape and structure since the maximal mass of water impinging on the airfoil is a function of freestream velocity. The friction heat term in the surface control volume is function of the freestream velocity: it increases with increasing velocity. Therefore, a higher surface temperature yields more runback water mass which corresponds to glaze ice conditions.

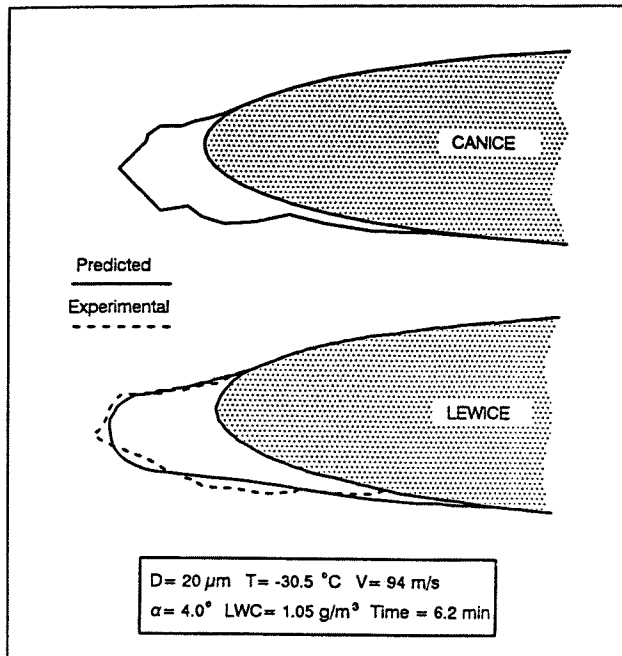


Figure 1: Comparison of Computed and Experimental Ice Shapes ( $T = -30.5^{\circ}C$ )

#### 7.1.4 Droplet Diameter

Droplets of higher diameter have an increased tendency to impinge on the body since higher inertia makes it more likely to deviate further from the streamlines and hit the body instead of avoiding it. Therefore, higher diameter droplets lead to an extended impingement region *i.e.* both impingement limits move further downstream, the catch efficiency peak increases and ice is formed aft of the ice protection systems (49).

### 7.2 Single-Element Airfoils

*CANICE* has been tested in rime and glaze ice conditions and compared with experimental data and numerical results. Figures 1 and 2 show comparison between results calculated with *CANICE* and those given by Shin *et al.* (50) in rime ice conditions. The calculated ice shape compares well with experimental data, particularly for the impingement limits on the upper and lower surface of the airfoil.

### 7.3 Multiple Element Configurations

Results for two multi-element airfoils are presented along with a comparison with numerical data obtained with an icing code developed at the *Centro Italiano Ricerche Aerospaziali* (CIRA, Italy) (51).

Calculations were performed on airfoils taken from Omar *et al.* (52). A two-element and four-element airfoils were chosen. The two-element airfoil is tested at lower velocity and lower temperature. The test

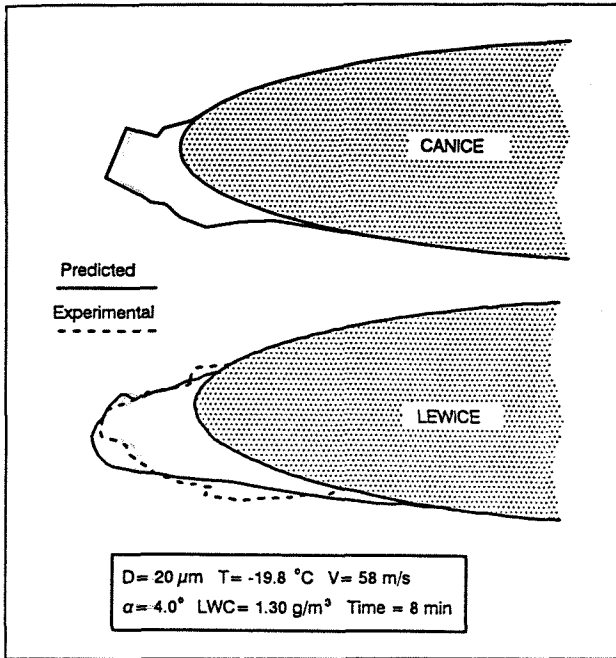


Figure 2: Comparison of Computed and Experimental Ice Shapes ( $T = -19.8^{\circ}\text{C}$ )

conditions are: zero incidence, airspeed of  $58\text{ m/s}$ , ambient temperature of  $-30^{\circ}\text{C}$ , liquid water content of  $1.05\text{ g/m}^3$ , mean equivolumetric diameter of  $20\text{ }\mu\text{m}$  and accretion time of  $300\text{ s}$ . These correspond to rime ice conditions. Results for the two-element airfoil are very similar for the main element although *CANICE-ME* predicted thicker ice on the trailing edge flap. Both the main element and flap have similar limit trajectory positions. The difference in thickness may reside in the thermodynamic analysis results.

For the four-element airfoil, the test conditions are: zero incidence, airspeed of  $94\text{ m/s}$ , ambient temperature of  $-8^{\circ}\text{C}$ , liquid water content of  $1.05\text{ g/m}^3$ , mean equivolumetric diameter of  $20\text{ }\mu\text{m}$  and accretion time of  $300\text{ s}$ . These correspond to glaze ice conditions. The resulting ice shapes predicted by both codes on the leading are very close. However, *CANICE-ME* predicts almost no ice on the first flap whereas the CIRA code predicts some fairly thick ice accretion. On the second flap, *CANICE-ME* predicts a very small ice thickness on the length of the underside which is similarly predicted by the CIRA code. The difference is the thickness at the leading edge of the flap. All these differences may come from the fact that the flow field is very complex and may not be well-predicted by either codes using a potential flow solver. To obtain better solutions, more complex flow field solvers would have to be used and implemented in icing codes. The four-element airfoil with high slat and flap deflection angles may well be the limit case for an icing code using a panel method.

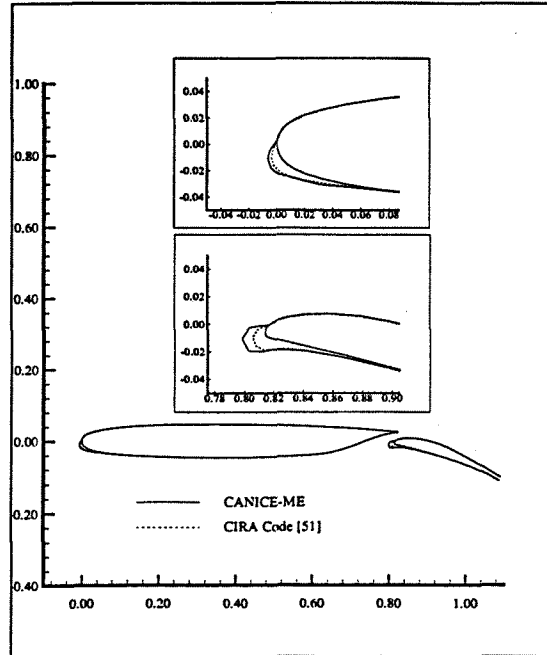


Figure 3: Icing on two-element airfoil ( $-30^{\circ}\text{C}$ ,  $58\text{ m/s}$ )

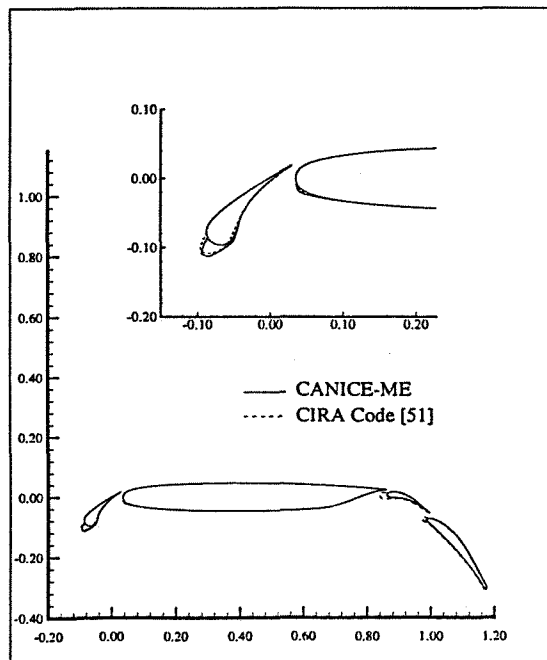


Figure 4: Icing on four-element airfoil ( $-8^{\circ}\text{C}$ ,  $94\text{ m/s}$ )

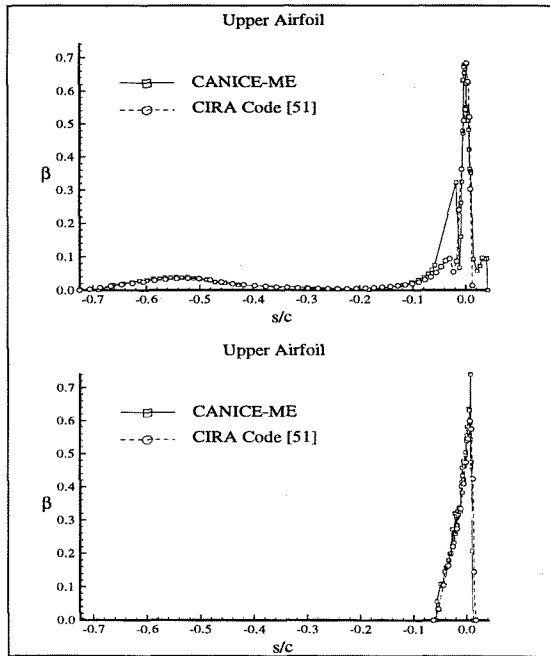


Figure 5: Comparison of local catch efficiency

#### 7.4 Nacelles

A nacelle was formed by opposing Benedek B7456D airfoils taken from reference <sup>(53)</sup>. It was tested numerically in icing conditions: zero and four degree incidence, airspeeds of 58 m/s and 94 m/s, ambient temperature of  $-30^{\circ}C$ , liquid water content of  $1.05\text{ g/m}^3$ , mean volume diameter of  $20\text{ }\mu\text{m}$  and an accretion time of 120 s. Fig. 5 shows comparison of local catch efficiency with numerical results obtained by CIRA. The results are very close with respect to both the tangent trajectories and the beta peaks. *CANICE-ME* calculates the local catch efficiency for each individual droplet impinging on the surface and it may help explain the second peak on the lower surface of the upper airfoil which is formed by a single point. Figs. 6 and 7 show both the complete view of the nacelle and zooms of the upper and lower airfoils for  $0^{\circ}$  and  $4^{\circ}$  degree incidence respectively, for a lower velocity of 58 m/s. Because of the shape of the airfoil, more ice appears on the exterior side. Figs. 8 and 9 show the resulting ice accretion on both airfoils for zero and four degree incidence and higher velocity of 94 m/s. For both velocities, at an incidence angle of  $4^{\circ}$ , some ice is formed in a second impact zone further downstream on the lower surface. This can be visualized on the beta curve of Fig. 5: there is a peak much further downstream. This is due to the geometry of the airfoil which is very much cambered and its nose is causing some shadowing effect.

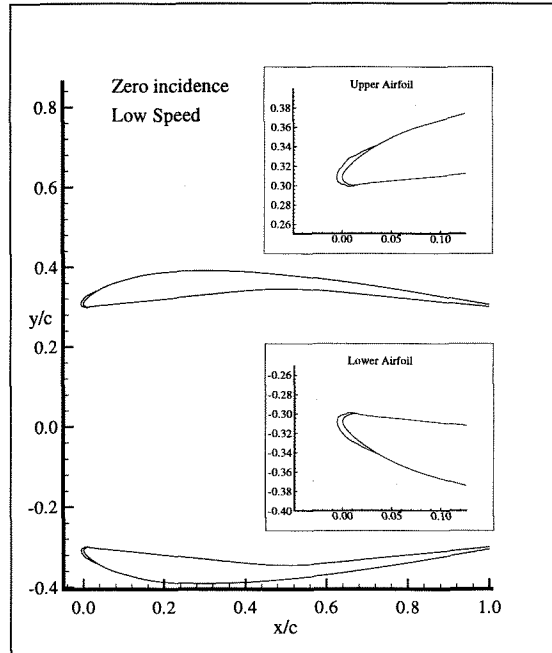


Figure 6: Ice accretion on nacelle ( $0^{\circ}$ , 58 m/s)

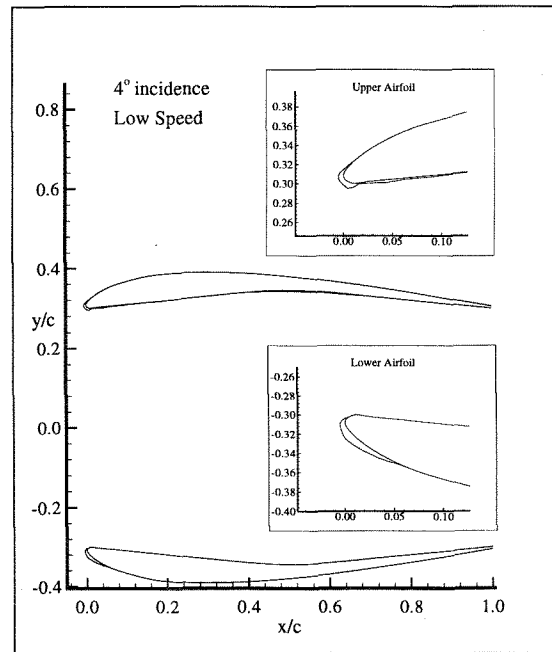


Figure 7: Ice accretion on nacelle ( $4^{\circ}$ , 58 m/s)

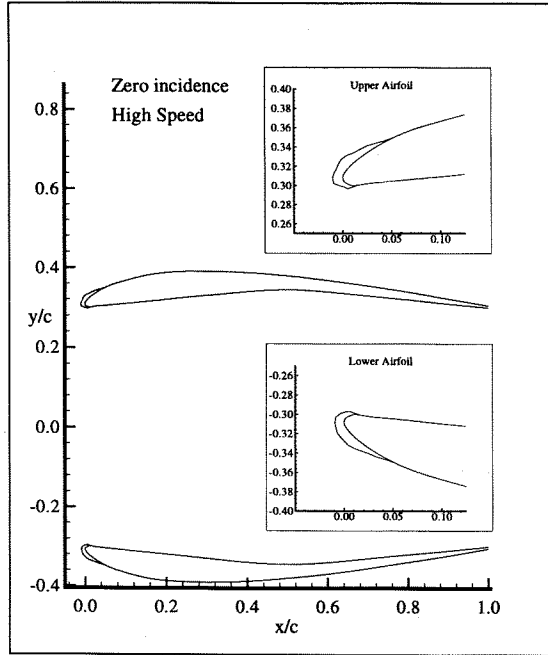


Figure 8: Ice accretion on nacelle ( $0^\circ$ ,  $94\text{ m/s}$ )

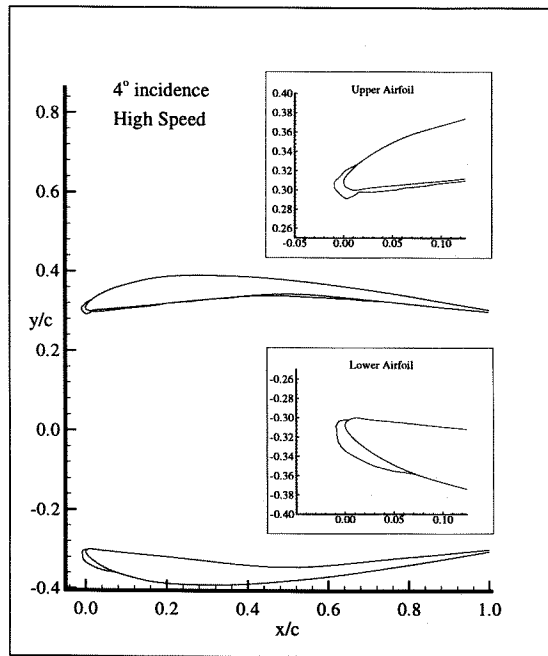


Figure 9: Ice accretion on nacelle ( $4^\circ$ ,  $94\text{ m/s}$ )

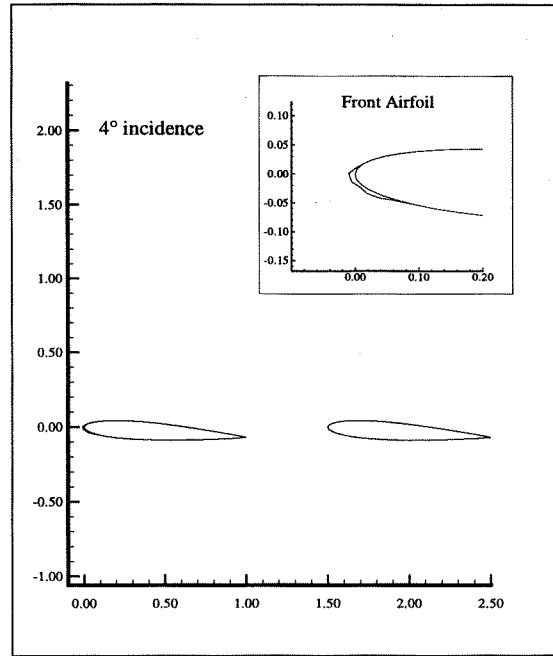


Figure 10: Icing on tandem airfoils ( $-10^\circ\text{C}$ ,  $94\text{ m/s}$ )

## 7.5 Airfoils in Tandem

Two NACA 0012 airfoils were placed in tandem at an incidence angle of  $4^\circ$ . The resulting ice accretion is presented in Fig. 10. No ice was detected on the rear airfoil since the front airfoil shields it from incoming water droplets. It was tested numerically in icing conditions: airspeed of  $94\text{ m/s}$ , ambient temperature of  $-10^\circ\text{C}$ , liquid water content of  $1.05\text{ g/m}^3$ , mean volume diameter of  $20\text{ }\mu\text{m}$  and an accretion time of  $300\text{ s}$ . The present test case was chosen to demonstrate *CANICE-ME* capabilities to predict ice accretion on any multiple body configurations.

## 7.6 Strake Wing

The strake planform shape is presented in Fig. 11. The wing has the following characteristics: incidence angle of  $5^\circ$ , semi-span of  $0.667$ , root chord of  $1.0$ , strake sweep angle of  $75^\circ$ , leading edge sweep angle of  $35^\circ$ , trailing edge sweep angle of  $9^\circ$  and a strake width of  $0.25$ .

The equivalent angle of attack method has been used to effect 2-D icing calculations on a 3-D wing. A 3-D panel method generated the sectional lift coefficients which are used for the 2-D icing calculation. Resulting ice accretions are presented in Fig. 11 for four different cross sections along the wing. The ice shapes are presented on the same scale to emphasize the change in chord length along the spanwise direction. The chosen icing conditions are: airspeed of  $58\text{ m/s}$ , ambient temperature of  $-10^\circ\text{C}$ , liquid water content of  $1.05\text{ g/m}^3$ , mean volume diameter of  $20\text{ }\mu\text{m}$  and an accretion time of  $120\text{ s}$ . We can observe



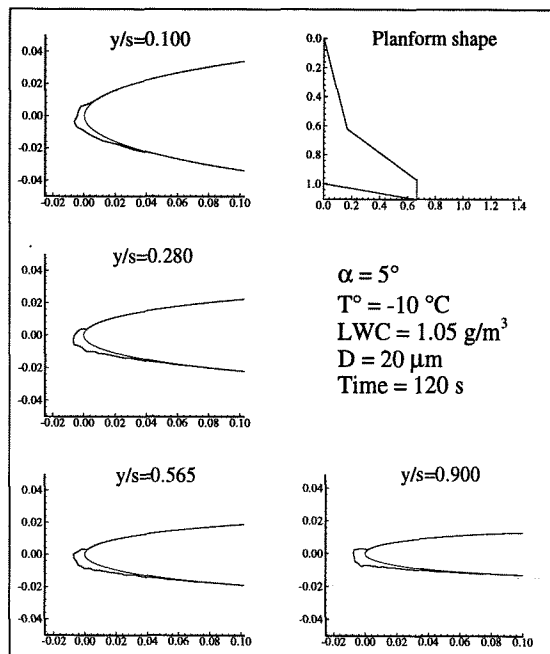


Figure 11: Ice accretion on strake wing

that the local catch efficiency increases with decreasing chord length.

## 8 Conclusions

An icing code capable of accommodating wings of any cross section or planform and 2-D nacelles has been successfully developed. Results obtained with the extension of *CANICE-ME* to accommodate multiple airfoil configurations and 3-D wings are promising.

To obtain a good icing simulation on nacelles, we will impose the mass flux of air coming through the airfoils. It would take into account blockage effects. The thermodynamic analysis could be replaced by a calculation module which would take into account the conduction through the wing skin, conduction between control volumes, and possibly de-icing/anti-icing thermal heating. This would enable the simulation of ice protection systems and accurately predict heat transfer requirements. This modelisation could be combined with the simulation of micro-physical aspects of ice formation such as: bead formation due to surface tension, rivulets movement, feather growth and impact angle considerations. Finally, to simulate a realistic ice accretion on aircraft wings we believe that the following points represent the most important areas where we could improve icing codes:

- Analyze the micro-physical aspects of ice accretion.
- Improve the correlations of equivalent sand-grain roughness.

- Develop an accurate model of convective heat transfer.
- Predict more accurately collection efficiency by improving the particle trajectory calculation using more complex flow field solvers.

In addition, supercooled large droplets (SLD), *i.e.* larger than  $40 \mu\text{m}$  which is the upper limit in the FAA certification envelope, have to be taken into account since they have been identified as a possible cause of some aircraft accidents such as the ATR-72 crash in 1994.

Once these aspects become well established then the prediction of performance degradation and analysis of controllability degradation could be handled. An extension of the performance prediction is to study the aeroelastic characteristics of the iced aircraft, *i.e.* the aircraft's responses to flutter, buffeting and other phenomena caused by fluid-solid interaction.

## Acknowledgements

This work was prepared in the context of J.-A. Bombardier Aeronautical Chair. The authors gratefully acknowledge the support provided by Bombardier Inc./Canadair. The authors would also like to thank Mr. Mingione from the *Centro Italiano Ricerche Aerospaziali* (CIRA, Italy) for exchanging some ice accretion data for comparison purpose.

## References

- (1) Green, S. "In-Flight Icing Certification Working Paper", International Icing Symposium '95, Montréal, Canada, September 18-21, 1995, pp. 401-411.
- (2) Mavriplis, F., "Icing and Contamination of Aircraft Surfaces: Industry's Concerns", Proceedings of the First Bombardier International Workshop on Aircraft Icing and Boundary-Layer Stability and Transition, Montréal, Sept. 20-21, 1993, pp. 51-55.
- (3) "Effects of Adverse Weather on Aerodynamics", AGARD Conference Proceedings CP-496, December 1991.
- (4) Federal Aviation Administration, "Large Aircraft Ground De-icing", Pilot Guide, US department of Transportation, AC 120-58, September 30, 1992.
- (5) Bergrun, N, "Warming Trend for Icing Research", Aerospace America, August 1995, pp 22-27.

- (6) Potapczuk, M.G. and Reinmann, J.J., "Icing Simulation: A Survey of Computer Models and Experimental Facilities", AGARD-CP-496, North Atlantic Treaty Organization, Toulouse, France, April 29th-May 1st, 1991, pp. 5.1-5.27.
- (7) Potapczuk, M.G., "Experimental Investigation of Multi-element Airfoil ice Accretion and Resulting Performance Degradation", Journal of Aircraft, August 1990, pp. 679-691.
- (8) Proceedings of the First Bombardier International Workshop on Aircraft Icing and Boundary-Layer Stability and Transition, Edited by I. Paraschivoiu, Montréal, Canada, September 20-21, 1993.
- (9) Reinmann, J.J., "NASA Aircraft Icing technology Program", NASA TM-104518, December 1991.
- (10) Gent, R.W., "Ice Accretion Prediction on Aerofoils", Proceedings of the First Bombardier International Workshop on Aircraft Icing and Boundary-Layer Stability and Transition, Montréal, Canada, September 20-21, 1993, pp. 113-138.
- (11) Hedde, T., "Modélisation tridimensionnelle des dépôts de givre sur les voilures d'aéronefs", Thèse de doctorat de l'Université Blaise Pascal, Clermont-Ferrand II, France, No d'ordre: D.U. 462, Décembre 1992.
- (12) Bragg, M.B., "Rime Ice Accretion and its Effects of Airfoil Performance", Ph.D. Dissertation, The Ohio State University, 1981 (also NASA CR 165599, March 1982).
- (13) Lozowski, E.P. and Oleskiw, M.M., "Computer Simulation of Airfoil Icing Without Runback", AIAA Paper 81-0402, January 1981.
- (14) Frost, W., Chang, H.P. and Kimble, K.R., "Particle Trajectory Computer Program for Icing Analysis", Final Report for NASA Lewis Research Center, Contract NAS3-22448, FWG Associates Inc., April 1982.
- (15) Cansdale, J.T. and Gent, R.W., "Ice Accretion on Airfoils in Two-Dimensional Compressible Flow - A Theoretical Model", Royal Aircraft Establishment, Technical Report 82128, 1983.
- (16) MacArthur, C.D., Keller, J.L. and Luers, J.K., "Mathematical Modeling of Ice Accretion on Airfoils", AIAA 20th Aerospace Sciences Meeting, January 11-14, 1982.
- (17) Bragg, M.B., "Predicting Rime Ice Accretion on Airfoils", AIAA Journal, Vol. 23, No 3, March 1985, pp. 381-387.
- (18) Flemming, R.J. and Lednicer, D.A., "High Speed Ice Accretion on Rotorcraft Airfoils", NASA CR-3910, August 1985.
- (19) Cebeci, T., "Effect of Environmentally Imposed Roughness on Airfoil performance", NASA CR-179639, June 1987.
- (20) Cebeci, T., "Calculation of Flow Over Iced Airfoils", AIAA Journal, Vol. 27, No. 7, July 1989, pp. 853-861.
- (21) Bragg, M.B. and Khodadoust, A., "Effect of Simulated Glaze Ice on a Rectangular Wing", AIAA Paper 89-0750.
- (22) Ruff, G.A. and Berkowitz, B.M., "User's Manual for the NASA Lewis Ice Accretion Prediction Code (LEWICE)", NASA CR-1851129, May 1990.
- (23) Cebeci, T., Chen, H.H. and Alemdaroglu, N., "Fortified LEWICE with Viscous Effects", Journal of Aircraft, Vol. 28, No. 9, September 1991, pp. 564-571.
- (24) Potapczuk, M.G., "LEWICE/E: An Euler Based Ice Accretion Code", AIAA Paper 92-0037.
- (25) Potapczuk, M.G., Al-Khalil, K.M. and Velazquez, M.T., "Ice Accretion and Performance Degradation Calculations with LEWICE/NS", AIAA Paper 93-0173.
- (26) Potapczuk, M.G., and Bidwell, C.S., "Numerical Simulation of Ice Growth on a MS-317 Swept Wing Geometry", NASA TM-103705, AIAA Paper 91-0263.
- (27) Wright, W.B., "Advancements in the LEWICE Ice Accretion Model", AIAA Paper 93-0171.
- (28) Kwon, O. and Sankar, L.N., "Numerical Investigation of Performance Degradation of Wings and Rotors Due to Icing", AIAA Paper 92-0412.
- (29) Hansman, R.J., "Microphysical Factors Which Influence Ice Accretion", Proceedings of the First Bombardier International Workshop on Aircraft Icing and Boundary-Layer Stability and Transition, Montréal, Canada, September 20-21, 1993, pp. 86-103.
- (30) Guffond, D., "Validation du programme bidimensionnel de captation", ONERA RT 20/5146 SY, May 1988.

- (31) Hedde, T. and Guffond, D., "Improvement of the ONERA 3D Icing Code, Comparison with 3D Experimental Shapes", AIAA Paper 93-0169.
- (32) Gent, R.W., "TRAJICE2 - A Combined Water Droplet trajectory and Ice Accretion Prediction Program for Aerofoil", DRA Technical Report TR90054, November 1990.
- (33) Brahim, M.T., Tran, P. and Paraschivoiu, I., "Numerical Simulation and Thermodynamic Analysis of Ice Accretion on Aircraft Wings", Centre de Développement Technologique de l'École Polytechnique de Montréal, C.D.T. Project C159, Final Report prepared for Canadair, May, 1994.
- (34) Guffond, D., "Le givrage des aéronefs", l'Aéronautique et l'Astronautique, No 148-149, 3-4, 1991, pp. 51-54.
- (35) Britton, R.K., "Computer Simulation of Airfoil Icing Without Runback", AIAA Paper 91-0661, January 1991.
- (36) Brumby, R.E., "The Effect of Wing Ice Contamination on Essential Flight Characteristics", AGARD-CP-496, December 1991, pp. 2-1 to 2-4.
- (37) Bragg, M.B., "Experimental Aerodynamic Characteristics of an NACA 0012 Airfoil with Simulated Glaze Ice", Journal of Aircraft, Vol.25, No. 9, September 1988, pp. 849-854.
- (38) Caruso, S.C., "NEARICE: An Unstructured-Mesh Navier-Stokes-Based Ice Accretion Prediction Method", AIAA Paper 94-0606.
- (39) Potapczuk, M.G., and Bidwell, C.S., "Numerical Simulation of Ice Growth on a MS-317 Swept Wing Geometry", NASA TM-103705, AIAA Paper 91-0263.
- (40) Cebeci, T. and Besnard, E., "Progress Towards the Prediction of the Aerodynamic Performance Degradation of an Aircraft in Natural Icing Conditions", Proceedings of the First Bombardier International Workshop, Montréal, September 20-21, pp. 56-85 (also AIAA Paper 94-0292).
- (41) Hess, J.L., Smith, A.M.O., "Calculation of Potential Flow About Arbitrary Bodies", Progress in Aeronautics Sciences, Vol. 8, pp.1-138, 1966.
- (42) Paraschivoiu, I., Tran, P. and Brahim, M.T., "Prediction of Ice Accretion with Viscous Effects on Aircraft Wings", AIAA Journal of Aircraft, Vol 31, No 4, July-Aug., 1994, (also AIAA Paper 93-0027).
- (43) Chen, H.H. and Cebeci, T. "Prediction of Ice Shapes on Wings and Multielement Airfoils, AIAA Paper 94-0608.
- (44) Messinger, B.L., "Equilibrium Temperature of an Unheated Icing Surface as a Function of Air Speed", Journal of the Aeronautical Sciences, January 1953, pp. 29-42.
- (45) Von Doenhoff, A.E. and Horton, E.A., "A Low Speed Experimental Investigation of the Effect of Sandpaper Type of Roughness on Boundary-Layer Transition", NACA TN 3858, 1956.
- (46) Shin, J., Berkowitz, B., Chen, H. and Cebeci, T., "Prediction of Ice Shapes and their Effect on Airfoil Performance", Journal of Aircraft, Vol 31, No 2, March-April, 1994, pp. 263-270, (also AIAA Paper 91-0264).
- (47) Tran, P., Brahim, M.T., Paraschivoiu, I., Pueyo, A. and Tezok, F., "Ice Accretion on Aircraft Wings with Thermodynamic Effects", Journal of Aircraft, Vol. 32, No. 2, March-April 1995, pp. 444-446. (also AIAA Paper 94-0605).
- (48) Olsen, W., Shaw, R. and Newton, J., "Ice Shapes and the Resulting Increase for NACA 0012 Airfoil", NASA TM 83556, 1984.
- (49) Brahim, M.T., Tran, P., Tezok, F. and Paraschivoiu, I., "Numerical Simulation of Aircraft Icing Due to Supercooled Large Droplets", FAA International Conference on Aircraft In-Flight Icing, Springfield, VA, May 6-8, 1996.
- (50) Shin, J., Berkowitz, B., Chen, H. and Cebeci, T., "Prediction of Ice Shapes and their Effect on Airfoil Performance", Journal of Aircraft, Vol 31, No 2, March-April, 1994, pp. 263-270, (also AIAA Paper 91-0264).
- (51) Amendola, A., Mingione, G. and Vicini, A., "Some Peculiar Aspects of an Icing Wind Tunnel Design: Large Droplets and Altitude Effects", Proceedings of the International Icing Symposium'95, Montréal, Canada, Sept. 18-21, 1995, pp. 267-278.
- (52) Omar, E., Zierten, T., Hahn, M., Szpiro, E. and Mahal, A., "Two Dimensional Wind Tunnel Test of a NASA Supercritical Airfoil with Various High-Lift Systems", NASA-CR-2215, Vol. II, 1973.
- (53) Simons, M., "Model Aircraft Aerodynamics", Argus Books, Third Edition, 1994.